ISSN 0020-4412, Instruments and Experimental Techniques, 2019, Vol. 62, No. 2, pp. 298–303. © Pleiades Publishing, Ltd., 2019.

LABORATORY TECHNIQUES

Experimental Setup of ac Thermoelectric Power Measurements in a Cryocooler PPMS System and Its Implementation to Superconductors, Topological Insulator, and Thermoelectric Materials[1]

K. Shrestha[a], M. Gooch[a], B. Lorenz[a], and C. W. Chu[a,b,*]

[a] *TCSUH and Department of Physics, University of Houston, Houston, Texas, 77204-5002 USA*

[b] *Lawrence Berkeley National Laboratory, Berkeley, California, 94720 USA*

**e-mail: cwchu@uh.edu*

Received July 11, 2018; revised July 11, 2018; accepted July 11, 2018

Abstract—We have designed and developed an experimental setup to measure the Seebeck coefficient of a variety of samples at cryogenic temperatures and under magnetic fields up to 7 T employing the physical property measurement system (PPMS). The measurement technique uses a low frequency ac thermal gradient generated by two thin film heaters in thermal contact with the sample. Heaters and temperature sensors are all fitted on a standard PPMS sample puck. The validity of this method is tested by measuring the thermoelectric power of several superconductors and thermoelectric samples. We have used this technique to measure the thermoelectric power of various topological insulator single crystals ($Pb_{0.8}Sn_{0.2}Te$, Bi_2Te_3, $Bi_2Se_{2.1}Te_{0.9}$, and Sb_2Te_3). The developed hardware and software control is suitable for studying the thermoelectric power of small samples (length 2 mm) in a commercial cryomagnetic system (PPMS) and it allows for studying superconductor, semiconductor, thermoelectric, or topological insulator material in wide temperature (2–300 K) and magnetic field (0–7 T) ranges.

DOI: 10.1134/S002044121902026X

1. INTRODUCTION

The Seebeck effect that describes the conversion of thermal energy into electrical energy has become a focus of study in many research areas, such as in thermoelectrics, superconductivity, and semiconductors [1–5]. It is also known as thermoelectric power or thermopower and is estimated by calculating the ratio of the thermoelectric voltage (ΔV) to the temperature gradient (ΔT) across the sample, i.e., $S = \Delta V/\Delta T$. This effect is the opposite of the Peltier effect [6], in which a temperature gradient arises across the sample if an electrical voltage is applied to it. The power factor (ZT), which is a dimensionless quantity, describes the efficiency of a thermoelectric material and is defined as $ZT = S^2\sigma T/k$, where S, σ, and k represent the Seebeck coefficient, electrical conductivity, and thermal conductivity, respectively. This implies that precise electrical and thermal transport measurements are crucial for estimating the power factor of thermoelectric materials. For simple semiconductors or single-band metals, the Seebeck coefficient is positive for the p-type and negative for the n-type conduction. Thus, the sign of the Seebeck coefficient could be taken as a preliminary probe to identify the nature of the bulk charge carriers, as a complement to Hall measurements. Since the electrical voltage of the sample is zero in the superconducting state, the Seebeck coefficient is zero and it can be used to identify the critical temperature in superconductivity research [7, 8]. Compared to electrical conductivity, the Seebeck coefficient is less sensitive to impurity or grain boundary scattering processes of charge carriers and thus provides a more accurate definition of the critical temperature of the superconducting state.

Recently, thermoelectric power under magnetic fields, magnetothermopower, has become a sensitive tool with which to study topological insulator, Dirac, and Weyl materials [9–14]. Thermoelectric power under high field also shows the quantum oscillations. By analyzing the oscillations, one can estimate the various physical parameters that characterize the Fermi surface and their topological nature. Thus, a precise magnetothermopower measurement setup would also be a useful tool for studying topological insulators, Weyl, and Dirac systems. Motivated by this, we have designed and adapted a Seebeck mea-

[1] The article is published in the original.

surement setup based on the dual heaters technique under magnetic fields to the physical properties measurement systems (PPMS, Quantum Design).

There are several techniques that are used for determining the thermoelectric power of a material [15–23]. However, ac thermoelectric power measurement technique is among the more popular due to its nearly perfect compensation of spurious dc voltages, fast measurements, and small temperature gradient along the sample [21–23]. Here, we present an experimental setup, based on the ac technique developed by Choi et al. [20], that can be used to measure precise thermoelectric power of a small sample in a broad temperature range (2–400 K) and under magnetic fields up to 7 T. Using this method, we have successfully measured the thermoelectric power of small (millimeter sized) single and polycrystalline samples of superconductor, thermoelectric, and topological insulator materials.

2. MEASUREMENT PRINCIPLE

The thermoelectric power measurement hardware was built on a sample puck for the PPMS and equipped with heaters, temperature sensors, and thermal reference point to implement a high precision ac technique as described by Choi et al. [20] The sample was placed across two sapphire plates (as shown in Fig. 1). A sinusoidal temperature gradient of chosen amplitude and frequency is created across the sample using two thin film heaters H_1 and H_2. For most measurements we choose a gradient of 0.25 K and a frequency of 0.1 Hz. A sinusoidal current is applied separately to the heaters H_1 and H_2 using two Keithley 220 programmable current sources with a 90° phase offset between them. The heater currents are adjusted before each measurement to maintain the same temperature gradient. If $I_1 = I_0\sin\omega t$ and $I_2 = I_0\cos\omega t$ (with I_0—amplitude and ω—angular frequency) are the current through H_1 and H_2, respectively, then total power

$$P = I^2R = I_1^2R + I_2^2R = I_0^2R \quad (1)$$

is constant with time. Here, R represents the heater resistance. This ensures that the average sample temperature is kept constant during the ac measurement.

A sinusoidal temperature gradient of 0.25 K at a frequency of 0.1 Hz is created and measured using the two thermocouples attached to the sample over a time of about 90 s simultaneously; the sinusoidal thermovoltage of the same frequency is measured across the sample. The amplitudes of both waves are estimated through a nonlinear curve fitting routine. The Seebeck coefficient is then estimated by calculating the ratio of the amplitude of thermovoltage (ΔV) to temperature gradient (ΔT), i.e., $S = \Delta V/\Delta T$. Like the lock-in technique, this fitting method eliminates significantly the noise in the measured data, allowing for a precise determination of the Seebeck coefficient [20].

The Seebeck measurements were performed in the PPMS (Quantum Design) in the 2–300 K temperature range. Figure 1a shows the sample configuration used in this study for the Seebeck measurements. As shown in the figure, a sample is mounted across the two wedge-shaped sapphire plates using GE varnish. The minimum distance between these sapphire plates is less than 1 mm, implying that any sample having a length on the mm order can be measured using this setup. Two thin film heaters (H_1 and H_2) are installed on the sapphire plates using GE varnish. The high thermal conductivity values of the sapphire and GE varnish ensure that the sample is in good thermal contact with the heaters. Two Keithley 220 current sources provide sinusoidal currents (I_1 and I_2) to H_1 and H_2 separately and create a sinusoidal temperature gradient of 0.25 K across the sample. The phase shift between the currents, I_1 and I_2, is 90°. Two constantan-copper thermocouples (TC_1 and TC_2) measure the temperature gradient across the sample. The open wires of both thermocouples are thermally anchored at a reference point on the puck so that only the temperature difference between this point and the spot on the sample is measured by each thermocouple. The TC reference consists of insulating thermal copper grease; thermocouple wires are embedded inside and held in place by pressing with a rectangular sapphire plate to ensure a homogeneous thermal environment. The temperature of the TC reference is measured by a Cernox (CX) temperature sensor embedded in the copper grease. The high thermal conductivity of copper grease ensures good thermal contact between the ends of the thermocouple wires and the CX temperature sensor. The temperature of each point on the sample where the thermocouples are attached is then measured by using the reference temperature from the CX thermometer and the thermovoltage of each thermocouple averaged over the 90 s measurement time. The sinusoidally changing thermoelectric voltage of the sample is collected during the 90 s measurement time (typically 1000 data points) using the two copper wires of the constantan-copper thermocouples and the differential input of the voltmeter. The overall circuit diagram of our experimental setup is displayed in Fig. 1b. Two programmable current sources (Keithley 220) provide the ac current to H_1 and H_2. There are two HP 34420A nanovoltmeters with two input channels each, one for measuring the voltage of thermocouples TC_1 and TC_2 (in Ch1 and Ch2) and another for measuring the sample's thermovoltage (in Ch1). The whole setup is built on the PPMS resistivity puck as sketched in Fig. 1c. Our modified PPMS puck is shown in Fig. 1d. The instruments and the puck are connected by the PPMS user bridge cable.

As shown in Fig. 1a, a HP 34420A nanovoltmeter measures the voltage across the copper wires Cu1 (of TC_1) and Cu2 (of TC_2) and the sample

$$V = V_{\mathrm{Cu1}} + V_{\mathrm{sample}} - V_{\mathrm{Cu2}}. \quad (2)$$

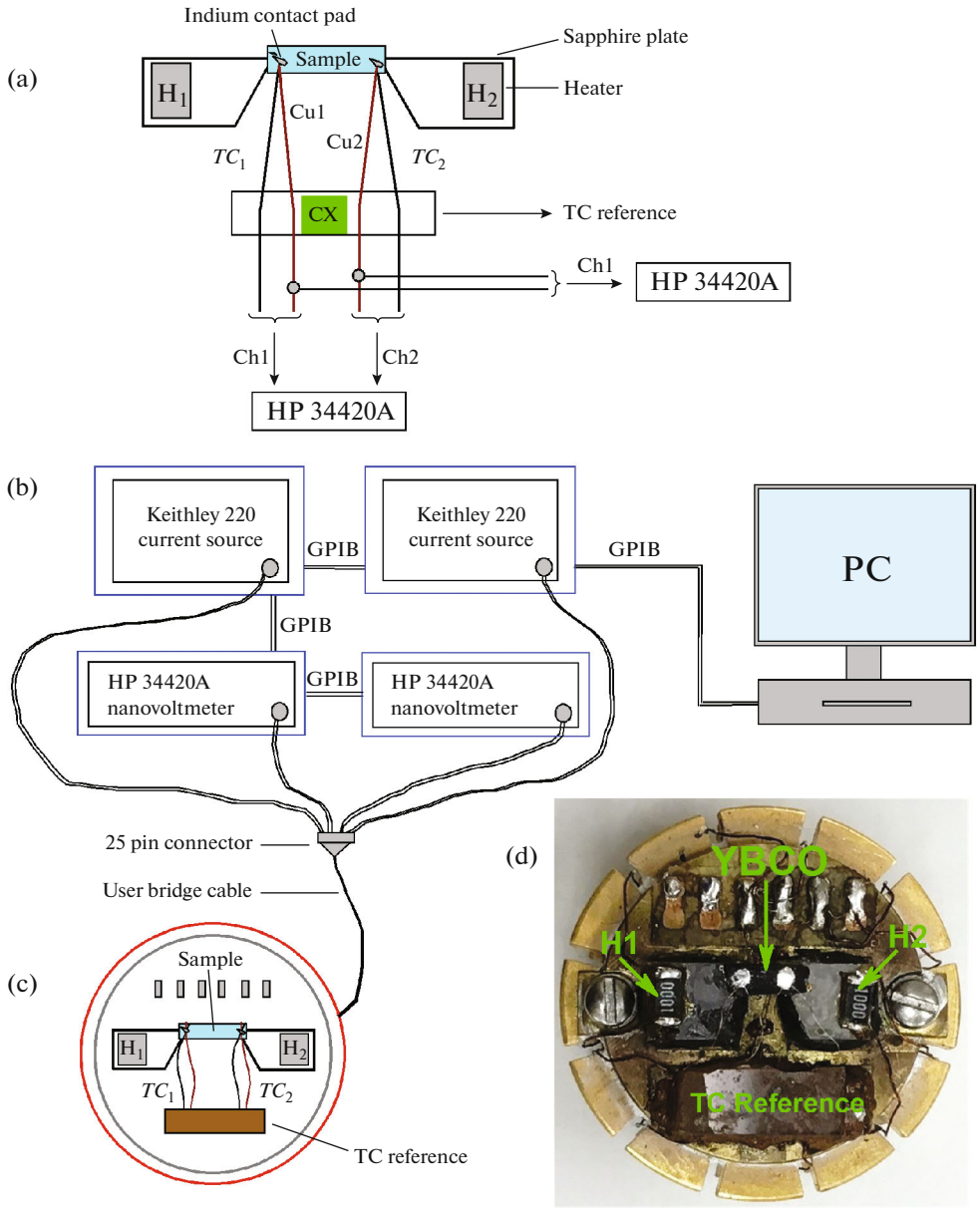

Fig. 1. (a) A schematic diagram of sample configuration for the Seebeck measurement. A sample is mounted on the sapphire plates. Two thermocouples TC_1 and TC_2 measure the temperature gradient across the sample. (b) The instruments setup for the thermoelectric power measurement. Two Keithley 220 current sources provide currents to the heaters (H_1 and H_2) to create the temperature gradient across the sample and a nanovoltmeter HP 34420A measures generated thermovoltage. (c) The sample mounting setup in the PPMS puck. (d) A photo of the modified PPMS puck (diameter 24 mm) in our setup showing the sample (YBCO), heaters (H_1 and H_2), and thermocouple reference. Two white patches on the sample surface are the indium contacts for holding two thermocouple wires (TC_1 and TC_2; see the text).

The measured thermoelectric voltage of the sample has to be corrected for the contribution of the copper wires used for measurement, Cu1 and Cu2. The thermoelectric voltage across the copper wires was calibrated by using an $YBa_2Cu_3O_7$ (YBCO) high temperature superconductor sample below its critical temperature; and at higher temperatures, high purity lead was employed, using the known thermoelectric power of lead.

For measurements in magnetic fields all thermometers and wires have to be calibrated to take into account any change of properties in magnetic fields. The CX temperature sensor at the reference point has a negligible field dependence up to the maximum field of 7 T. This was tested in a careful measurement after stabilizing the PPMS temperature and varying the external field. However, the constantan-copper thermocouples show a field dependence that cannot be

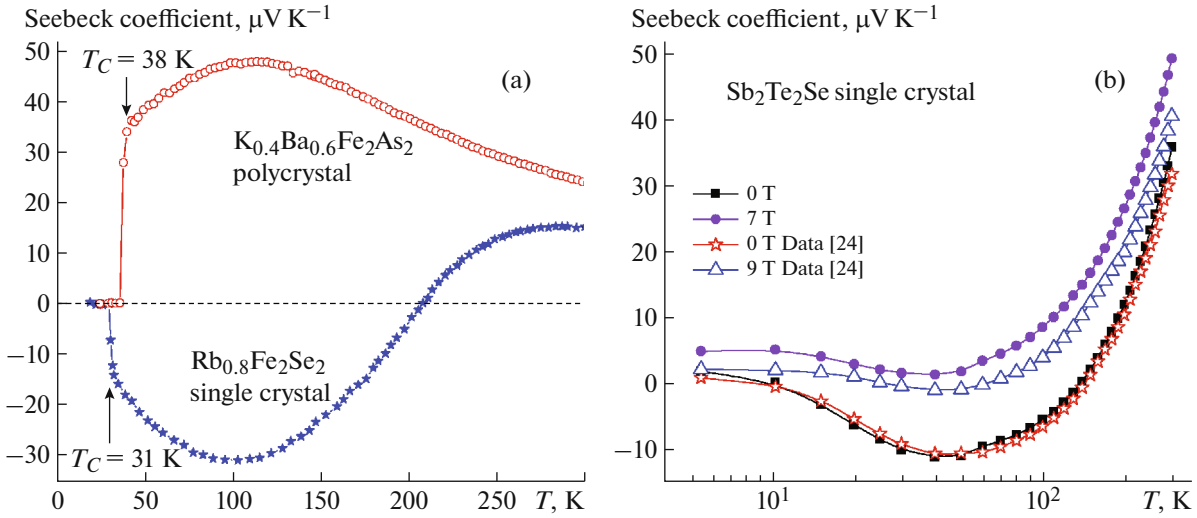

Fig. 2. (a) Temperature dependence of the Seebeck coefficient of $K_{0.4}Ba_{0.6}Fe_2As_2$ polycrystal and $Rb_{0.8}Fe_2Se_2$ single crystal samples. The superconducting transition temperatures, T_C = 31 K and 38 K are shown by the arrows. (b) Temperature dependence of the Seebeck coefficient for the Sb_2Te_2Se single crystal at 0 T (solid rectangle) and 7 T (solid circle). The open symbols (star—0 T, triangle—9 T) represent previously reported data [24] obtained using the TTO option in PPMS (Quantum Design).

neglected. They have been calibrated by applying a constant temperature gradient between the junction and the reference point using one of the thin film heaters. The response of the thermocouple was monitored until the temperature gradient in zero magnetic field became stationary and constant with time. The value of the applied current was adjusted such a way that it creates a constant temperature gradient of 0.5 K. The field correction to the thermoelectric voltage of the constantan-copper thermocouples was then measured at different magnetic field values and a numerical routine was developed to apply the correction in any future measurement. Similarly, the magnetic field dependence of thermovoltage across the copper wires Cu1 and Cu2 was carried out using a manganin foil as the reference sample. The thermoelectric power and its field dependence of the manganin foil had been calibrated previously by employing the thermal transport option (TTO) of the PPMS. The field correction of the copper wires has been implemented in the software controlling the measurement process and evaluating the thermoelectric signal of the sample to be measured. A nonlinear curve fitting procedure was used to determine the amplitude of both the thermal gradient and the thermoelectric voltage across the sample from the corresponding sinusoidal responses. The PPMS temperature controller is used to control the sample temperature. The instruments, including PPMS, are interconnected by the GPIB interface and data are collected in the computer using the Visual Basic program. All the measurements were performed in high vacuum, typically 10^{-6} Torr.

3. MEASUREMENT RESULTS

The experimental setup and algorithm were tested in zero magnetic field by measuring two known superconducting materials, $Rb_{0.8}Fe_2Se_2$ single crystal and $K_{0.4}Ba_{0.6}Fe_2As_2$ polycrystal [25, 26]. The data are shown in Fig. 2a. $Rb_{0.8}Fe_2Se_2$ shows a positive Seebeck coefficient at room temperature that turns negative with decreasing temperature below T = 210 K. However, $K_{0.4}Ba_{0.6}Fe_2As_2$ shows a positive Seebeck coefficient over the whole temperature range. For both samples, the thermopower shows a sudden jump to zero at the critical temperatures of T_C = 31 K and 38 K, respectively. These transition temperatures are consistent with the corresponding resistivity measurements [25, 26].

The thermoelectric power and its field dependence were measured for several topological systems. Sb_2Te_2Se is a good thermoelectric compound and its topological insulator nature has recently been proven by both experimental and theoretical studies [27, 28]. Figure 2b presents the Seebeck measurements at different temperatures in a semi-log plot for a Sb_2Te_2Se single crystal that was used in our previous study [28]. The Seebeck value at T = 300 K is S = 35 V K^{-1}; it decreases with temperature and changes sign to negative at T = 140 K. However, it returns to the positive with further decrease in temperature below T = 10 K. The thermopower value in our measurements is consistent with previous data [24] (see Fig. 2b). In order to investigate the influence of magnetic fields, we have measured the thermopower of Sb_2Te_2Se under 7 T of applied field. The Sb_2Te_2Se sample shows a positive magneto-thermopower and follows a similar temperature depen-

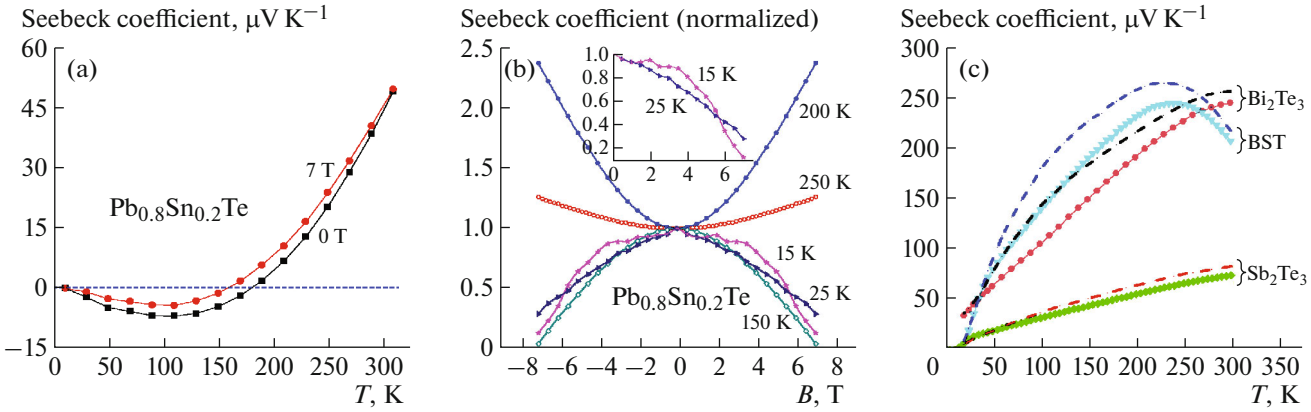

Fig. 3. (a) Temperature dependence of the Seebeck coefficient for a $Pb_{0.8}Sn_{0.2}Te$ single crystal under magnetic fields of 0 and 7 T. (b) Magnetic field dependence of the Seebeck coefficient of a $Pb_{0.8}Sn_{0.2}Te$ single crystal at different temperatures. The curvature of the Seebeck curve changes while lowering the temperature below $T = 200$ K. Inset: Low temperature (15 and 25 K) curves showing a signature of quantum oscillations at higher fields. (c) Temperature dependence of the Seebeck coefficient for Bi_2Te_3, $Bi_2Se_{2.1}Te_{0.9}$ (BST), and Sb_2Te_3 single crystals under magnetic fields of 0 (symbols with lines) and 7 T (dashed lines).

dence as that previously measured at 9 T (the blue dashed line in Fig. 2b). It is important to note that the magnetothermopower of our Sb_2Te_2Se sample at 7 T is higher than that in the previous report [24] at 9 T. The magnetic field response of a sample depends on its crystalline quality. Thus, the higher magnetothermopower of our sample could be due to its better crystalline quality [residual resistivity ratio (RRR) = 3.5] as compared to the sample used in [24] (RRR = 2.3).

From the thermopower measurements of the superconducting and topological samples, we have shown the validity of our experimental approach. We thus proceeded to implement this technique for other topological systems. Figure 3a shows the temperature dependence of the Seebeck coefficient of a $Pb_{1-x}Sn_xTe$ ($x = 0.2$) single crystal. Theoretical and experimental studies have confirmed that $Pb_{1-x}Sn_xTe$ undergoes a topological phase transition (topologically trivial to non-trivial) at a critical doping level $x_c = 0.25$ [29, 30]. Here, we have measured the thermoelectric power of $Pb_{1-x}Sn_xTe$ ($x = 0.2$) just below the critical doping. At room temperature, the value of the Seebeck coefficient is measured to be $S = 50$ V K^{-1}. The S value decreases with temperature and becomes negative below $T = 180$ K. Its absolute value decreases with further decrease in temperature and becomes nearly zero at $T = 10$ K. The $Pb_{1-x}Sn_xTe$ ($x = 0.2$) sample shows a positive magnetothermopower under the magnetic field of 7 T. We have also studied the magnetic field dependence of the Seebeck coefficient. Figure 3b shows the normalized Seebeck coefficient, $S(B)/S(0)$, of a $Pb_{1-x}Sn_xTe$ ($x = 0.2$) single crystal at different temperatures. The Seebeck coefficient shows the parabolic (upward) dependence on the magnetic field. The sign of curvature changes (upward to downward) as the temperature is lowered below $T = 200$ K. This is because of the sign change of the thermopower value around that temperature. It should be noted that at low temperatures (15 25 K), there is a signature of quantum oscillations at higher fields as shown in the inset to Fig. 3b. Higher magnetic fields (beyond the current field range up to 7 T) are needed to resolve these oscillations and study their properties. Similarly, Fig. 3c shows the thermopower of the single crystals Bi_2Te_3, $Bi_2Se_{2.1}Te_{0.9}$ (BST), and Sb_2Te_3 at zero and 7 T applied fields. The topological nature of these compounds has already been confirmed by our previous measurements [31–35]. All of the above samples show the positive magnetothermopower. The data obtained on the topological samples here can be used to estimate various physical parameters characterizing the system using the Mott relation [36] (see [12] and references therein).

4. SUMMARY

In this work, we have adapted the ac technique for the precise measurement of the Seebeck coefficient of small samples to the Physical Property Measurements System for temperature and magnetic field control. Using this experimental setup, we have successfully measured the thermoelectric power of various topological insulator and superconducting compounds in cryogenic temperatures and in strong magnetic fields. The novelty of this experimental setup is that it is applicable to a very small (2 mm in length) and very thin (0.1 mm) sample of any shape, which might not be possible in other experimental techniques, such as the TTO option in PPMS (Quantum Design), in magnetic fields up to 7 T. Measurements of various samples, including iron pnictide superconductors and topological insulator compounds, in a wide temperature range and in magnetic fields have been presented.

These results validate the developed hardware and prove the high precision of the method.

ACKNOWLEDGMENTS

This work is supported in part by the U.S. Air Force Office of Scientific Research Grant FA9550-15-1-0236, the T.L.L. Temple Foundation, the John J. and Rebecca Moores Endowment, and the State of Texas through the Texas Center for Superconductivity at the University of Houston.

REFERENCES

1. DiSalvo, F.J., *Science,* 1999, vol. 285, p. 703. doi 10.1126/science.285.5428.703
2. Bell, L., *Science,* 2008, vol. 321, p. 1457. doi 10.1126/science.1158899
3. Cyr-Choinire, O., Badoux, S., Grissonnanche, G., Michon, B., Afshar, S.A.A., Fortier, S., LeBoeuf, D., Graf, D., Day, J., Bonn, D. A., Hardy, W. N., Liang, R., Doiron-Leyraud, N., and Taillefer, L., *Phys. Rev. X,* 2017, vol. 7, p. 031042. doi 10.1103/PhysRevX.7.031042
4. Tapp, J.H., Tang, Z., Lv, B., Sasmal, K., Lorenz, B., Chu, P.C.W., and Guloy, A.M., *Phys. Rev. B,* 2008, vol. 78, p. 060505. doi 10.1103/PhysRevB.78.060505
5. Goldsmid, H. and Sharp, J., *J. Electron. Mater.,* 1999, vol. 28, p. 869. doi 10.1007/s11664-999-0211-y
6. Martin, J., Tritt, T., and Uher, C., *J. Appl. Phys.,* 2010, vol. 108, p. 121101. doi 10.1063/1.3503505
7. Lv, B., Deng, L., Gooch, M., Wei, F., Sun, Y., Meen, J. K., Xue, Y.Y., Lorenz, B., and Chu, C.W., *Proc. Natl. Acad. Sci. U. S. A.,* 2011, vol. 108, p. 15705. doi 10.1073/pnas.1112150108
8. Gofryk, K., Griveau, J.-C., Riseborough, P.S., and Durakiewicz, T., *Phys. Rev. B,* 2016, vol. 94, p. 195117. doi 10.1103/PhysRevB.94.195117
9. Hor, Y., Qu, D., Ong, N., and Cava, R.J., *J. Phys.: Condens. Matter,* 2010, vol. 22, p. 375801. doi 10.1088/0953-8984/22/37/375801
10. Matusiak, M., Cooper, J., and Kaczorowski, D., *Nat. Commun.,* 2017, vol. 8, p. 15219. doi 10.1038/ncomms15219
11. Qu, D.-X., Hor, Y.S., and Cava, R.J., *Phys. Rev. Lett.,* 2012, vol. 109, p. 246602. doi 10.1103/PhysRevLett.109.246602
12. Liang, T., Gibson, Q., Xiong, J., Hirschberger, M., Koduvayur, S.P., Cava, R., and Ong, N., *Nat. Commun.,* 2013, vol. 4, p. 2696. doi 10.1038/ncomms3696
13. Stockert, U., Reis, R., Ajeesh, M.O., Watzman, S.J., Schmidt, M., Shekhar, C., Heremans, J.P., Baenitz, C.M., and Nicklas, M., *J. Phys.: Condens. Matter,* 2017, vol. 29, p. 325701. doi 10.1088/1361-648X/aa7a3b
14. Fauque, B., Butch, N.P., Syers, P., Paglione, J., Wiedmann, S., Collaudin, A., Grena, B., Zeitler, U., and Behnia, K., *Phys. Rev. B,* 2013, vol. 87, p. 035133. doi 10.1103/PhysRevB.87.035133
15. Zhou, Z. and Uher, C., *Rev. Sci. Instrum.,* 2005, vol. 76, p. 023901. doi 10.1063/1.1835631
16. Rouleau, O. and Alleno, E., *Rev. Sci. Instrum.,* 2013, vol. 84, p. 105103. doi 10.1063/1.4823527
17. Ponnambalam, V., Lindsey, S., Hickman, N.S., and Tritt, T.M., *Rev. Sci. Instrum.,* 2006, vol. 77, p. 073904. doi 10.1063/1.2219734
18. Liu, J., Zhang, Y., Wang, Z., Li, M., Su, W., Zhao, M., Huang, S., Xia, S., and Wang, C., *Rev. Sci. Instrum.,* 2016, vol. 87, p. 064701. doi 10.1063/1.4952744
19. Fu, Q., Xiong, Y., Zhang, W., and Xu, D., *Rev. Sci. Instrum.,* 2017, vol. 88, p. 095111. doi 10.1063/1.4990634
20. Choi, E.S., Brooks, J.S., Qualls, J.S., and Song, Y.S., *Rev. Sci. Instrum.,* 2001, vol. 72, p. 2392. doi 10.1063/1.1353192
21. Resel, R., Gratz, E., Burkov, A.T., Nakama, T., Higa, M., and Yagasaki, K., *Rev. Sci. Instrum.,* 1996, vol. 67, p. 1970. doi 10.1063/1.1146953
22. Freeman, R.H. and Bass, J., *Rev. Sci. Instrum.,* 1970, vol. 41, p. 1171. doi 10.1063/1.1684751
23. Kettler, W.H. and Rosenberg, M., *Rev. Sci. Instrum.,* 1986, vol. 57, p. 3053. doi 10.1063/1.1139195
24. Wang, K., Graf, D., and Petrovic, C., *Phys. Rev. B,* 2014, vol. 89, p. 125202. doi 10.1103/PhysRevB.89.125202
25. Gooch, M., Lv, B., Deng, L.Z., Muramatsu, T., Meen, J., Xue, Y.Y., Lorenz, B., and Chu, C.W., *Phys. Rev. B,* 2011, vol. 84, p. 184517. doi 10.1103/PhysRevB.84.184517
26. Gooch, M., Lv, B., Lorenz, B., Guloy, A.M., and Chu, C.W., *J. Appl. Phys.,* 2010, vol. 107, p. 09. doi 10.1063/1.3362932
27. Lin, H., Das, T., Wray, L.A., Xu, S.-Y., Hasan, M.Z., and Bansil, A., *New J. Phys.,* 2011, vol. 13, p. 095005. doi 10.1088/1367-2630/13/9/095005
28. Shrestha, K., Marinova, V., Graf, D., Lorenz, B., and Chu, C.W., *Phys. Rev. B*, 2017, vol. 95, p. 075102. doi 10.1103/PhysRevB.95.075102
29. Tanaka, Y., Sato, T., Nakayama, K., Souma, S., Takahashi, T., Ren, Z., Novak, M., Segawa, K., and Ando, Y., *Phys. Rev. B,* 2013, vol. 87, p. 155105. doi 10.1103/PhysRevB.87.155105
30. Gao, X. and Daw, M.S., *Phys. Rev. B,* 2008, vol. 77, p. 033103. doi 10.1103/PhysRevB.77.033103
31. Shrestha, K., Marinova, V., Lorenz, B., and Chu, P.C.W., *Phys. Rev. B,* 2014, vol. 90, p. 241111. doi 10.1103/PhysRevB.90.241111
32. Shrestha, K., Chou, M., Graf, D., Yang, H.D., Lorenz, B., and Chu, C.W., *Phys. Rev. B,* 2017, vol. 95, p. 195113. doi 10.1103/PhysRevB.95.195113
33. Shrestha, K., Graf, D.E., Marinova, V., Lorenz, B., and Chu, C.W., *Philos. Mag.,* 2017, vol. 97, p. 1740. doi 10.1080/14786435.2017.1314563
34. Shrestha, K., Marinova, V., Graf, D., Lorenz, B., and Chu, C.W., *J. Appl. Phys.,* 2017, vol. 122, p. 125901. doi 10.1063/1.4998575
35. Shrestha, K., Graf, D., Marinova, V., Lorenz, B., and Chu, C.W., *J. Appl. Phys.,* 2017, vol. 122, p. 145901. doi 10.1063/1.4997947
36. Ziman, J.M., *Electrons and Phonons: The Theory of Transport Phenomena in Solids,* Oxford: Clarendon Press, 1960.